Chemical Reviews

Volume 78, Number 3 June 1978

The Photoexcited Triplet State and Photosynthesis†

HAIM LEVANON‡ and JAMES R. NORRIS*

Radiation Laboratory and Department of Chemistry, University of Notre Dame, Notre Dame, Indiana 46556, and Chemistry Division, Argonne National Laboratory, Argonne, Illinois 60439

Received September 26, 1977

Contents

I. Introduction

Photosynthesis (PS) is the process in which solar energy is converted into chemical potential energy by plants and certain bacteria. Generally speaking PS can be represented by the Van Neil reaction[1,2]

$$CO_2 + 2H_2A \xrightarrow{h\nu} CH_2O + H_2O + 2A \qquad (1)$$

Since PS represents the fundamental source of all energy available today,[3] it is remarkable that the basic energy conversion is not yet well understood. Thus, it is the ultimate goal of many laboratories to gain a closer insight into the basic principles and mechanisms of PS. A complete understanding of reaction 1 may ultimately lead to the elimination of carbon dioxide resulting in "simpler" processes such as

$$H_2O \xrightarrow{h\nu} H_2 + \tfrac{1}{2}O_2 \qquad (2)$$

PS can be divided into two types of mechanisms depending on the host organism: (a) green plants that evolve oxygen by oxidizing water and reducing carbon dioxide, (b) anerobic bacteria that cannot evolve oxygen by oxidizing water. All PS may be further divided into two main subcategories: (a′) light-induced reactions and (b′) dark reactions. The processes a′ and b′ are coupled together via series of electron transfer reactions involving identified and unidentified intermediates. For purposes of discussion we shall arbitrarily define the primary act as the initial light-induced photochemical and photophysical changes that occur in times shorter than approximately 2×10^{-5} s.

How can one describe these initial light-induced processes? It is easier to demonstrate it first on bacterial PS which involves only one cyclic stage. The radiant energy is absorbed in or transferred, via antenna pigments (AP), to a basic unit known as the reaction center (RC). These antenna pigments consist mainly of bacteriochlorophylls (Bchl) and carotenoids (Car). It is primarily the former constituent that is photoexcited and responsible for the energy transfer to the RC (the conventional nomenclature for the bleached species in Bchl RC is P_{870}; P and 870 stand for pigment and the absorption wavelength, respectively). It is generally accepted that the reaction center contains the complex $(Bchl)_4$, two molecules of bacteriopheophytin (Bph), and a quinone–iron complex [Q–Fe].[4,5]

The primary photophysical processes in bacterial PS can be represented by eq 3. The photochemistry begins when each

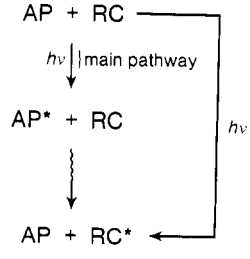

(3)

excited RC unit undergoes the following one-stage, electron-transfer processes.

(a) An electron ejection from two molecules in $[Bchl]_4$ to an intermediate electron acceptor A (time scale,[6,7] ~6 ps):

$$\{Bchl\}_4^* + A \rightarrow \{Bchl\}_2 + \{Bchl\}_2^{\cdot+} + A^{\cdot-} \qquad (4)$$

† The research described herein was supported by the Office of Basic Energy Science of the Department of Energy. This is Document No. SR-40 from the Notre Dame Radiation Laboratory.

* Authors to whom inquiries should be sent either at the Hebrew University (H.L.) or at Argonne National Laboratory (J.R.N.).

‡ On leave from the Department of Physical Chemistry, the Hebrew University, Jerusalem, Israel.

0009-2665/78/0778-0185$05.00/0

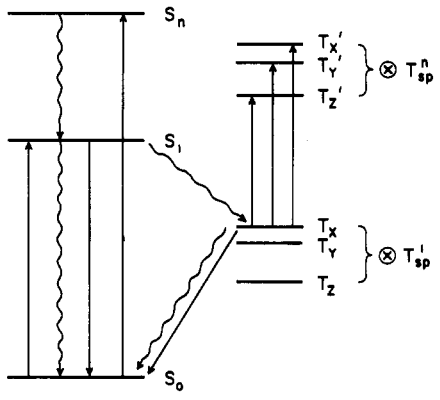

Figure 1. A simplified representation of Jablonski diagram. The singlet and triplet manifolds are represented by S and T, respectively. The vibrational structure is omitted. The spatial parts in the triplet manifold are represented by T_{sp}^1 and T_{sp}^n. The spin parts are represented by T_x, T_y, T_z for the first excited triplet and T_x, T_y', T_z' for the *n*th excited triplet. For convenience we refer to the direct product of the spatial and spin state as T_{i1} or T_{in}. We have assumed that the principal axes in the upper triplet state may be oriented differently from those in the lowest triplet, such that the spin parts do not necessarily coincide for the two states. Straight arrows indicate either absorption or emission of photons, and the wiggled arrows represent radiationless transitions. The particular transitions are discussed in the text.

There is no conclusive evidence for the identification of A which is interpreted by some authors as a Bph species.[7-9] Reaction 4 is normally referred to as the pre-primary or intermediate electron-transfer (charge separation) process.[8,9]

Much of the forthcoming discussion in bacterial PS will be focussed on the identity of P_{870} as a special pair of Bchl molecules. The original special pair model was based primarily on interpretation of EPR line-shape data.[10] Confirmation by ENDOR demonstrated that the cation signal associated with the primary donor of PS is delocalized over two approximately equivalent Bchl molecules.[11,12] In green plants, P_{700} was also interpreted as a special pair composed of two Chl a molecules.[10-12] Various structural models, not always complementary, have been proposed for this in vivo special pair. Some of them will be discussed in the subsequent section.

(b) Secondary electron transfer occurring to a [Q-Fe] complex[13] (time scale,[6,7] ~250 ps):

$$A^{\cdot -} + \{Q\text{-}Fe\} \rightarrow A + \{Q\text{-}Fe\}^{\cdot -} \qquad (5)$$

(c) The following electron transfer flow proceeding via cytochrome b and cytochrome c_2 completing the cycle via the reaction (time scale,[14] ~10 μs):

$$\{Bchl\}_2^{\cdot +} + \text{cytochrome } c_2(Fe^{2+}) \rightarrow \{Bchl\}_2 + \text{cytochrome } c_2(Fe^{3+}) \qquad (6)$$

Reactions 4-6 describe only the photochemistry following the primary act. The subsequent biochemical reactions are not described here but are associated with the dark reactions. In oxygen evolving PS, the photophysical and photochemical processes are more complicated. This type of PS probably involves two photosystems, I and II, and is generally described in terms of the Z scheme.[4] In this case the AP capture energy for two different types of RC (RC_I and RC_{II}) is reflected by eq 7. RC_I

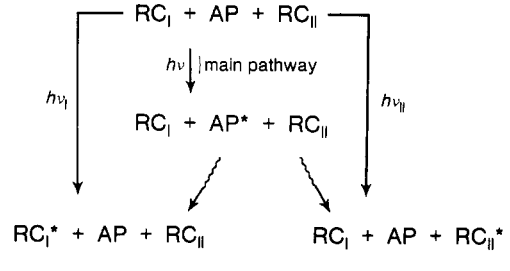

(7)

uses energy of red light quanta to reduce carbon dioxide whereas RC_{II} is responsible for the oxidation of water with concomitant evolution of oxygen.

The AP in photosystem I is believed to consist mainly of Chl a and Car, while the AP of photosystem II consists mainly of Chl a and Chl b. The corresponding changes in absorption occurring in photosystem I are at 700 nm and are attributed to Chl a pigments, P_{700}, which is considered to be the primary donor special pair.[4,10] Regarding the intermediate stages, analogous to those described by eq 4-6, the experimental data are scarce and sometimes contradictory. Nevertheless, bacterial PS can be applied with appropriate modifications to photosystem I in oxygen evolving PS. The photophysics and photochemistry of photosystem II are more complicated and less defined than either photosystem I or bacterial PS. There is, however, some evidence that the bleaching at 680 nm is due to Chl a which is considered to be the primary donor, P_{680}, in photosystem II.[15] It is noteworthy that Chl a in oxygen evolving PS and Bchl a in bacterial PS are the most important pigments in subsequent processes such as light harvesting, channeling the excitation energy to the RC, and participating in the first step of charge separation. Thus, the common feature in all the above systems is that the primary events in PS are proceeding via energy-rich intermediates such as singlets, doublets, triplets, and radical pairs. Some of these transients may affect other existing paramagnetic states such as high- and low-spin Fe complexes as well as high-spin Mn complexes.

A. Physical Description of Photoexcited States

We discuss basic properties of photoexcited states in terms of the Jablonski diagram given in Figure 1.[16,17] In this energy level diagram are shown only the ground and low excited states in the singlet, and triplet, manifolds and the typical transitions between them. The existing higher spin multiplicities, quartets, triplets, etc., will not be discussed in this survey.

In a unimolecular photophysical act we distinguish between the following common processes: (a) radiative excitation which results in absorptive transitions:

$S_n \leftarrow S_0$	spin allowed
$S_1 \leftarrow S_0$	spin allowed
$S_{n>1} \leftarrow S_1$	spin allowed
$T_1 \leftarrow S_0$	spin forbidden
$T_n \leftarrow T_1$	spin allowed

(b) radiative deexcitation which results in luminescence transitions:

$S_1 \rightarrow S_0$	spin allowed (fluorescence)
$T_1 \rightarrow S_0$	spin forbidden (phosphorescence)
$T_n \rightarrow T_1$	spin allowed (triplet fluorescence)

(c) radiationless transitions between isoenergetic levels of different states:

$S_n \rightsquigarrow S_1$	internal conversion
$S_1 \rightsquigarrow S_0$	radiationless deactivation
$T_n \rightsquigarrow T_1$	internal conversion
$S_1 \rightsquigarrow T_1$	intersystem crossing
$T_1 \rightsquigarrow S_0$	intersystem crossing

Two earlier reviews[18,19] have not emphasized the general physical details of the triplet state in PS. Moreover, during the past 2 years, important new experimental and theoretical studies relevant to the triplet state in PS have become available. Thus,

in this survey we intend to provide the reader with a more recent physical description of the primary events of PS that may involve the triplet state. The controversial question whether a photoexcited triplet state is involved directly or indirectly in PS has not yet been settled. However, there is little doubt that this paramagnetic intermediate serves as a probe for studying the structure and mechanism of the primary act, and information revealed by spectroscopy of the triplet state in PS is not easily provided by other methods. Except for the triplet state and its relation to PS, most of the transient stages in PS have been treated recently.[5,20] Other aspects of primary stages in PS as well as a complete coverage of the biochemical and biophysical processes are beyond the scope of this survey and the reader is referred to recent literature.[5,21,22]

This review attempts to cover the 1975–1977 period. We have mainly emphasized those aspects which can be investigated by magnetic resonance spectroscopy. Because of the large volume of literature in this period, we may have unintentionally neglected some important work which should have been included; for this we apologize.

II. Detection of the Photoexcited Triplet State

A. Optical Spectroscopy

We will discuss results of optical spectroscopy that involve the triplet state either directly or indirectly, and in general deal with the overall spectral changes that are photoinduced by an actinic light source. Some of the spectral changes result directly from photoproduction of an excited triplet state, such as triplet–triplet absorption ($T_n \leftarrow T_1$) and phosphorescence ($T_1 \rightarrow S_0$). In all cases the optical changes are considered to be associated with transients and thus must be recorded as a function of time as well as wavelength.

The most frequently encountered direct optical detection of the triplet state for our purpose is absorption rather than emission. Many of the compounds of interest do not phosphoresce (or phosphoresce very weakly). In order to measure absorption changes, difference spectroscopy must be employed.[23] Always a "dark" reference spectrum must be obtained in which the monitoring light is sufficiently weak so as not to perturb the system itself. The "light" spectrum may be obtained with an intense actinic light which strongly perturbs the sample. In order to obtain the net transient spectrum, a substractive process of some type must be employed. In the simplest method the intense light may also serve as a monitoring beam with the monochromator placed after the sample. However, a better experimental configuration involves separate perturbing and monitoring light sources, i.e., flash[24] or laser photolysis.[24] In the latter case both lights can be monochromatic at different wavelengths and with appropriate time profiles. The "action" spectrum of the intense actinic light can then be obtained as well as the optical spectrum of the species produced by the actinic source. The ability of pulsing or amplitude modulating both sources, especially the actinic source, is desired in order to obtain kinetic information or to identify photoexcited species of different lifetimes. The application of conventional flash and laser photolysis techniques in PS studies suffers from the main disadvantage of relatively low resolution times, i.e., ~10 μs and ~10 ns, respectively. Recently, time resolution of a few picoseconds has become possible using advanced laser spectroscopy.[6,7,25] The primary advantages of optical absorption spectroscopy are high time resolution and high sensitivity. In many instances the main disadvantage is low optical resolution and the inability to identify uniquely the source of the absorption changes.

In addition to absorption, luminescence may be monitored after light excitation of the sample. Again, for the systems of interest here, the luminescence is typically fluorescence and not phosphorescence. The mechanism resulting in the fluorescence can be of a photochemical as well as a photophysical nature. Although luminescence will not be emphasized in this review, the reader should be aware of the possible photochemical origin of luminescence and its possible implication for the triplet state in PS.

B. Optical Magnetic Resonance Spectroscopy

1. Spin Hamiltonian and Triplet Dynamics at Zero Magnetic Field

In the previous section we outlined some optical methods for observing the triplet state. The first excited triplet state, T_1, in most cases, is comprised of three nondegenerate spin sublevels. Thus a more detailed analysis of the appropriate transitions within the triplet manifold is required. The major experimental technique is optical magnetic resonance (OMR) which can be further subdivided into optical detection of magnetic resonance (ODMR)[26] and optical electron paramagnetic or nuclear magnetic resonance spectroscopy (OEPR)[27] or (ONMR),[28] respectively. The former experiments are normally performed in the absence of an external magnetic field at very low temperatures, whereas the latter experiments are performed at high magnetic fields over a wide range of temperatures.

Consider a typical organic triplet state which is formed via intersystem crossing (ISC) from the singlet manifold. The degeneracy removal in the absence of an external magnetic field is mainly due to the dipolar interaction between the two unpaired electrons:[29]

$$\mathcal{H}_d = \mathbf{S} \cdot \hat{\mathbf{D}} \cdot \mathbf{S} \tag{8}$$

where $\mathbf{S}$ is the spin operator and $\hat{\mathbf{D}}$ is the dipolar tensor operator which is traceless and transforms like a second-rank spherical tensor. Expansion of (8) gives rise to different representations of the dipolar Hamiltonian. For example, in terms of a coordinate system which diagonalizes the dipolar tensor:

$$\mathcal{H}_d = -(XS_x^2 + YS_y^2 + ZS_z^2) \tag{9}$$

where X, Y, and Z are the expectation values of the principal axes between the spatial wave functions:

$$\begin{aligned} X &= -\frac{1}{2} g^2\beta^2 \left\langle \frac{r^2 - 3X^2}{r^5} \right\rangle \\ Y &= -\frac{1}{2} g^2\beta^2 \left\langle \frac{r^2 - 3Y^2}{r^5} \right\rangle \\ Z &= -\frac{1}{2} g^2\beta^2 \left\langle \frac{r^2 - 3Z^2}{r^5} \right\rangle \end{aligned} \tag{10}$$

Since $X + Y + Z = 0$, eq 9 can be replaced by another common representation:

$$\mathcal{H}_d = D[S_z^2 - {}^1/_3 S^2] + E[S_x^2 - S_y^2] \tag{11}$$

where D and E are the zero-field splitting (ZFS) parameters, which are expressed in terms of X, Y, and Z:

$$\begin{aligned} D &= -{}^3/_2 Z \\ E &= {}^1/_2 (Y - X) \end{aligned} \tag{12}$$

To solve the dipolar spin-Hamiltonian at zero magnetic field it is convenient to employ the zero-field wave functions $\tilde{T} \equiv |T_x\rangle$, $|T_y\rangle$, $|T_z\rangle$. The resulting energy levels are shown in Figure 1. Some useful aspects can be enumerated at this point regarding the dipolar Hamiltonian.

a. The ZFS parameters and the corresponding energy levels depend strongly on the average distance between the two unpaired electrons (molecular dimensions) in the photoexcited triplet (eq 10).

b. The absolute signs of D and E depend on the particular choice of coordinate system. Usually, D and E are assigned such that $|D| > 3|E|$.

c. The molecular symmetry should affect the ZFS parameters. In cubic symmetry where all three principal axes are equivalent, both $|D|$ and $|E|$ vanish leaving a completely degenerate system at zero field. In molecules of lower symmetry where a fourfold symmetry exists, the $|E|$ value vanishes leaving a partial degeneracy at zero field. When a small rhombic contribution is introduced, $|D|$ and $|E|$ are nonvanishing, thus lifting completely the degeneracy at zero field.

d. The ZFS parameters range approximately between 0.1 and 0.01 cm^{-1} and are thus amenable to microwave frequency spectroscopy.

Before explaining in somewhat more detail the ODMR technique, we first consider requirements for ODMR and illustrate them for zero-field ODMR since this is the most frequently encountered situation. ODMR primarily depends on ISC that produces significant deviations from Boltzman populations of the three spin eigenstates T_x, T_y, T_z at zero magnetic field. The singlet state carries no spin angular momentum whereas the triplet state does. Thus, when a singlet–triplet transition occurs, spin angular momentum of the system necessarily changes. Such a change requires a special mechanism. In most situations the mechanism for ISC involves spin–orbit coupling giving rise to nonvanishing matrix elements of the type $\langle S|\mathcal{H}_{so}|T\rangle$.[30] The spin–orbit Hamiltonian is proportional to the scalar product **L·S**, where **L** is the orbital angular momentum operator and **S** is the spin angular momentum operator. Simply stated, changes in orbital angular momentum provide torques that create or destroy spin angular momentum. The triplet sublevels at zero field are defined in a molecular axis system and thus are highly "anisotropic". Likewise, the change in orbital angular momentum which provides the magnetic torque necessary to "flip" the spin in ISC is highly anisotropic. In systems of a single symmetry, the coupling between the first excited singlet and first excited triplet state is given by

$$\langle S_1|\mathcal{H}_{so}|T^1_{sp}\,T_i\rangle \equiv \langle S_1|\mathcal{H}_{so}|T_{i1}\rangle \qquad (13)$$

for $i = x, y, z$, T^1_{sp} is the spatial orbital of the triplet state, T_i is the triplet spin state, and S_1 is the first excited singlet state. From symmetry considerations the nonvanishing matrix elements must obey the general relation[30]

$$\Gamma(\text{triplet orbital}) \otimes \Gamma(\text{triplet spin}) = \Gamma(\text{singlet orbital}) \qquad (14)$$

where Γ is the irreducible representation of the corresponding point group. The case where only a single triplet spin sublevel T_{x1} is connected to the singlet manifold is illustrated in Figure 1. This type of spin–orbit coupling is responsible for three types of ISC processes:

$$S_1 \rightsquigarrow T_{x1}\ (\text{ISC})$$
$$T_{x1} \rightsquigarrow S_0\ (\text{radiative decay phosphorescence}) \qquad (15)$$
$$T_{x1} \rightsquigarrow S_0\ (\text{nonradiative decay}) \qquad (15)$$

Such a description breaks down in the real world because several states of different symmetries can be involved, but in general (perhaps always) ISC is highly selective with respect to the three spin sublevels predominantly populating only a single level or a pair of levels in significant excess to the remaining levels or level. The ISC rates at zero field will be proportional to the square of maxtrix elements of the type:[31]

$$\begin{aligned} &|\langle S_1|\mathcal{H}_{so}|T^1_{sp}\,T_i\rangle|^2 \text{ for population rates } A_i \\ &|\langle S_0|\mathcal{H}_{so}|T^1_{sp}\,T_i\rangle|^2 \text{ for depopulation rate } k_i \end{aligned} \qquad (16)$$

2. Optical Detection of Magnetic Resonance Experiments at Zero Field

ODMR is a simple and elegant technique for observing magnetic resonance in the photoexcited triplet state.[26] In this approach, an optical parameter of the system under study, for example, phosphorescence, is monitored as a function of microwave frequency and/or power. The method involves at least double resonance conditions, namely one of optical energy ($\geq \sim 10^4$ cm^{-1}) and one of microwave energy (0.1 to 0.01 cm^{-1}). In most cases the optical property may be fluorescence ($S_1 \rightarrow S_0$),[32] phosphorescence ($T_{i1} \rightarrow S_0$),[33-35] or triplet–triplet absorption ($T_{in} \leftarrow T_{i1}$),[36] where $i = x, y, z$. At conditions where double resonance occurs a change in microwave power affects the intensity of the optical properties and vice versa.

Now we would like to describe, using our example in Figure 1, how the population of the three triplet sublevels can be manipulated in such a manner as to change the population in the ground and first excited singlet and in the triplet state. In order to do this we will first assume that no coupling within the T_{i1} manifold occurs in the absence of external microwave radiation. From Figure 1 it should be clear that the population of the ground state S_0 after optical light excitation depends on the lifetime of the triplet state. This is true for steady-state optical light flux as well as pulsed light excitation. In our example the triplet lifetime is controlled only by T_{x1} with the lifetime of T_{y1} and T_{z1} set to infinity (in the absence of a coupling by microwave with T_{x1}). It is easy to see that this triplet lifetime could be detected by monitoring triplet–triplet absorption or phosphorescence with no magnetic resonance involved. However, much more information becomes available when any optical property of the system is monitored while applying microwaves in resonance with the three possible energy gaps shown in Figure 1 (i.e., $T_{x1} \rightarrow T_{y1}$, $T_{x1} \rightarrow T_{z1}$, or $T_{y1} \rightarrow T_{z1}$). In the case of Figure 1 only $T_{x1} \rightarrow T_{y1}$ or $T_{x1} \rightarrow T_{z1}$ are initially effective since no initial population is shown in T_{y1} or T_{z1}. If saturating microwave (CW or pulsed) is applied to $T_{x1} \leftarrow T_{y1}$ or $T_{x1} \rightarrow T_{z1}$, then $N_{T_{x1}} \cong N_{T_{y1}}$ or $N_{T_{x1}} \cong N_{T_{z1}}$ where $N_{T_{i1}}$ is the population of a sublevel T_{i1}. In other words, approximately half the initial T_{x1} triplets are transferred to T_{y1} or T_{z1}, and thus the number of molecules available to return to S_0 is halved. Since the number of molecules returning to S_0 is reduced, N_{S_0} and N_{S_1} decrease. Experimentally, this can be observed in both $S_1 \leftarrow S_0$ absorption changes as well as in $S_1 \rightarrow S_0$ fluorescence changes. Also, phosphorescence is decreased and ultimately triplet–triplet absorption $T_{jn} \leftarrow T_{i1}$ will be changed. The $T_{x1} \rightarrow T_{y1}$ or $T_{x1} \rightarrow T_{z1}$ is a resonance condition, and thus the triplet energy gaps are determined by monitoring any of the three above-mentioned optical measurements as a function of microwave frequency. Since the technique of ODMR depends on significant deviations from Boltzmann populations within the three spin sublevels produced by highly selective ISC rates, it is preferable if these deviations are preserved. The communication between the triplet sublevels is controlled by spin lattice relaxation (SLR) times which are highly temperature dependent. At temperatures between 1 and 2 K the SLR times of the system approach the triplet lifetime. Thus ODMR requires very low temperatures, which may be considered as the main limitation of this technique.

Since ODMR is typically performed at <2 K, SLR is absent and kinetics of the triplet state are simplified. In principal the observed time response is due to only the ISC rate parameters A_i and k_i ($i = x, y, z$). The time response can be measured by pulsing either the microwaves or the light, but typically the microwaves are pulsed. The kinetic parameters that are obtained by this method depend on the intensity of the light and must be extrapolated to sufficiently low light flux in order to obtain correct results.[37,38] In terms of kinetic response, ODMR has the time resolution and sensitivity of optical spectroscopy although in general the perturbing microwave pulses are in the nanosecond region.

3. Spin Hamiltonian in a Magnetic Field: EPR Experiments

In a magnetic field the photoexcited triplet energy levels will become field dependent as shown by Figure 2. The spin-Ham-

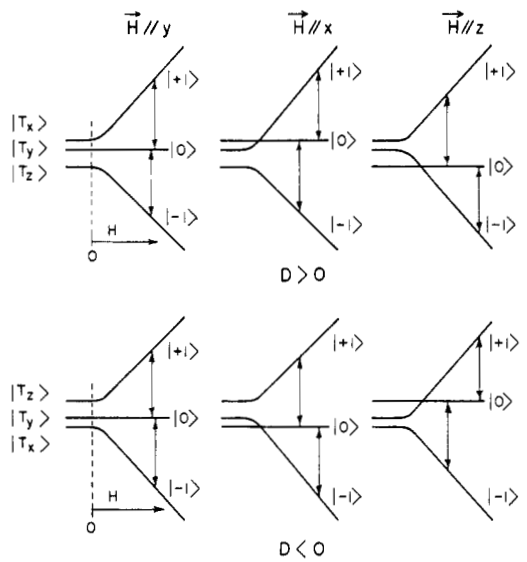

Figure 2. Magnetic field dependence of the spin energy levels for the three canonical orientations. The upper trace is the energy level diagram for $D > 0$, whereas the lower trace is for $D < 0$. The high-field wave functions are transformed to the zero field wave functions via the inverse matrix in eq 19. The $|0\rangle \leftrightarrow |-1\rangle$ and $|0\rangle \leftrightarrow |+1\rangle$ transitions for each canonical orientation will be defined as $1i$ and $2i$ ($i = x, y, z$), respectively. Thus, the six $\Delta M = \pm 1$ transitions in the direction from low field to high field will be $(2z)(1x)(1y)(2y)(2x)(1z)$ for the upper trace and $(1z)(2x)(2y)(1y)(1x)(2z)$ for the lower trace.

iltonian must now include the Zeeman term[39]

$$\mathcal{H} = \beta \mathbf{H} \cdot \hat{\mathbf{g}} \mathbf{S} + \mathcal{H}_d \tag{17}$$

where $\hat{\mathbf{g}}$ is a second rank tensor where in many cases its isotropic value almost coincides with the free electron g_e factor 2.0023. The detailed analysis of the Hamiltonian will not be treated here except for summarizing the useful and relevant points.[29]

a. Electron paramagnetic resonance (EPR) spectroscopy covers transition energies of the order of 0.3–1 cm^{-1} compared to 10^4–5×10^7 cm^{-1} in the optical spectroscopy methods described above. In addition, the conspicuous variation of EPR line widths reflects dynamic processes which may be studied over a wide range of times, i.e., 10^{-4}–10^{-10} s. These two properties make the EPR method very powerful in the unique determination of molecular structure and many inter- and intramolecular dynamic processes.

b. When the external magnetic field is along one of the principal axes, one state remains always stationary with respect to the field strength. The other two states diverge in opposite directions as the magnetic field increases (cf. Figure 2).

c. Accordingly, the spin wave functions will transform from zero-field wave functions $\tilde{T}$ to field-dependent wave functions. The high-field spin wave functions are $\tilde{n} \equiv |1\rangle, |0\rangle, |-1\rangle$ and are related to the zero-field wave functions through the transformation.

$$\tilde{T} = \tilde{n}R \tag{18}$$

where R is the matrix:

$$R = \begin{bmatrix} \frac{1}{\sqrt{2}} & \frac{i}{\sqrt{2}} & 0 \\ 0 & 0 & 1 \\ -\frac{1}{2} & \frac{i}{\sqrt{2}} & 0 \end{bmatrix} \tag{19}$$

d. It is the magnitude of $|D|$ and $|E|$ which determines whether one should be able to apply EPR spectroscopy to detect the triplet state. Thus, a necessary condition for EPR triplet detection is that the ZFS parameters $|D|$ and $2|E|$ should be

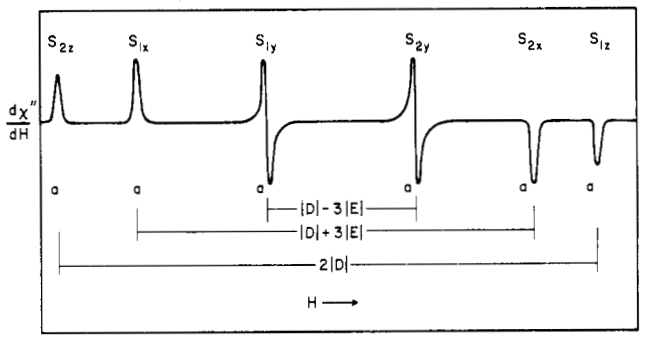

Figure 3. First derivative of a randomly oriented triplet having $|D| > 3|E|$. The line shape and peak intensities are typical of a triplet state that is in thermal equilibrium; i.e., all signal intensities are in the absorption mode indicated by *a*. The signal intensities S_{pi} ($p = 1, 2$ and $i = x, y, z$) are labeled according to the definitions given in the caption of Figure 2.

smaller than the external magnetic field. For a particular canonical orientation three transitions are possible: two at $\Delta M_s = \pm 1$ and one at the so called $\Delta M_s = \pm 2$.[40]

For a molecule with $|D| \neq |E| \neq 0$, it is evident from Figure 2 that the overall EPR transitions around $g_e \sim 2$ ($\Delta M_s = \pm 1$) will be 6. These transitions should be observed by conventional EPR detection; i.e., the microwave field is polarized perpendicular to the external magnetic field direction. The excursion of this spectrum will be $2|D|$ centered around the free electron g_e factor.

e. In oriented single crystals the search for and analysis of the triplet EPR spectra are performed in the $\Delta M_s = \pm 1$ region, where the EPR transitions are most intense. This type of analysis, however, cannot be carried out with compounds that could not be grown into oriented single crystals. This is the case in many porphyrin[41] and chlorophyll molecules in vitro and certainly in most biochemical preparations. Fortunately, much of this information can be derived by studying randomly oriented triplet states.[42] Considering the $\Delta M_s = \pm 1$ region, because of the anisotropy in the magnetic parameters, there is finite transition probability for each value of the magnetic field. It can be shown, however,[17] that the EPR transition at a magnetic field parallel to one of the principal axes is well defined in the randomly oriented first-derivative EPR spectrum. In a randomly oriented sample the three orientations are normally referred to as the canonical orientations. A characteristic feature of such a triplet spectrum is the occurrence of an additional transition to those already mentioned above. It appears at around $g \sim 4.0$ (1500 G for a ~9-GHz microwave frequency).[40]

Figure 3 demonstrates schematically a conventional $\Delta M_s = \pm 1$ EPR spectrum[43] of randomly oriented triplets. The line shape is typical of molecules with a rhombic contribution such that $|D| > 3|E| \neq 0$. It is also shown how the ZFS parameters can be evaluated from this type of spectrum. For molecules of axial symmetry (x and y principal axes are indistinguishable), $|E|$ vanishes. This results in the coalescence of S_{px} and S_{py} peak intensities (for the same pi) in the EPR spectrum.

f. As mentioned above the absolute sign of D and E depends on the choice of a molecular axis system. Conventional EPR detection prevents the sign determination from the experimental high-temperature triplet spectrum. However, the application of the magnetophotoselection (MPS)[44,45] method enables one to determine the signs of the ZFS parameters. This method can be applied to randomly oriented triplets whose triplet EPR spectra show distinct peaks at the canonical orientations. It is evident that these unique peaks are magnetically selected. On the other hand, the populating transitions $S_1 \leftarrow S_0$ are polarized according to the type of transition (e.g., $\pi^* \rightarrow \pi$ or $\pi^* \rightarrow$ n). By using plane-polarized light one can select the electric field transition, and subsequently the peak intensities in the canonical orienta-

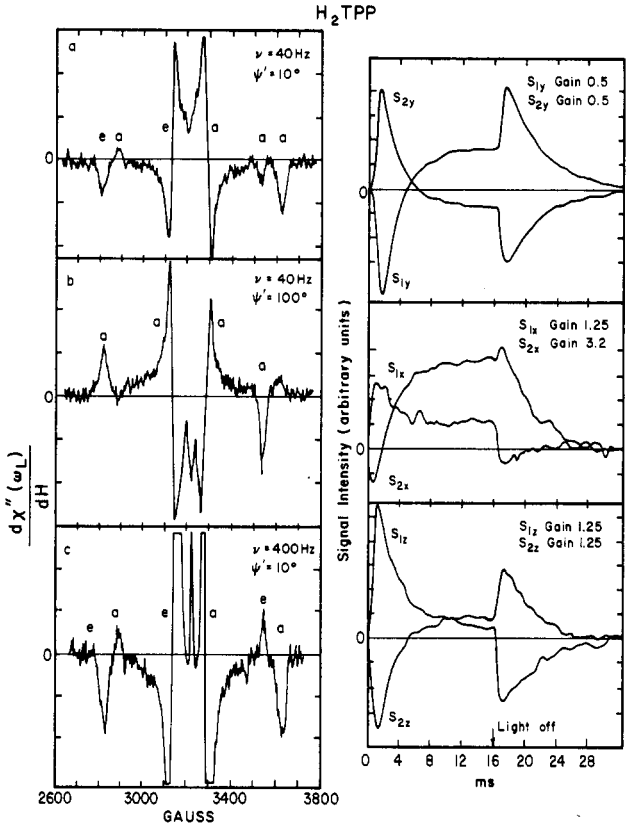

Figure 4. Left-hand side: first harmonic representation of triplet EPR spectrum of H_2TPP at different light modulation frequencies ν and phase angles ψ'. The lower trace spectrum was taken at high light modulation frequencies and the ESP pattern is indicated by the transients emission (e) or absorption (a). Right-hand side: kinetic curves for each canonical orientation describing the birth (light pulse on) and decay (light pulse off) of the signal intensity. The direction of the fast transients indicates the ESP patterns of the triplet spectrum. For details see ref 51. Notice that the canonical orientations x and y have been interchanged from the original presentation[51] to meet with the definitions described in Figure 2 (taken with permission from ref 51).

tions will be affected accordingly. Thus, if the polarization of the optical transitions with respect to the molecular framework are known, one can study the magnetic transitions or vice versa.

g. We summarize this section by reminding the reader that EPR triplet detection is performed at low temperatures[46] and in the solid-state phase (oriented single crystals, or randomly oriented molecules). The low-temperature requirement is to increase the sensitivity (Boltzmann factor) and to prevent additional deactivation processes which will shorten the triplet lifetime to such an extent that the steady-state concentration of the triplet will be too small to detect. The second requirement,[47] i.e., the solid state, is due to the relatively large values of the ZFS parameter (in terms of molecular reorientation correlation times) which prevent a complete averaging of the dipolar interaction, giving rise to broad EPR lines. Also, fast tumbling will result in very short SLR times as to produce severe line broadening so that the triplet EPR spectrum in solution would escape detection.

4. Triplet Dynamics by EPR Method

We have described above the feature of a steady-state triplet EPR spectrum (Figure 3), and how the magnetic parameters can be evaluated from it. As in ODMR, EPR technique enables one to elucidate details concerning the dynamics associated with the triplet manifold. The main requirement is that the kinetic parameters (population, depopulation, SLR rates) should lie within the time resolution and sensitivity of the detection apparatus.[27]

In the high-field approximation and for $|D| \ll g\beta H$,[48] the ISC rates are given by[31]

$$\langle \pm 1|k_{\pm}|\pm 1\rangle = 1/2(k_j + k_k)$$
$$\langle 0|k_0|0\rangle = k_i \qquad \text{for } i||H,\ i = x, y, z \tag{20}$$

The same relations hold for the population rate constants A_0 and $A_{\pm 1}$. For the other two perpendicular orientations, the rates are obtained using cyclic permutation. From eq 16 and 20 it follows that the ISC rates are not necessarily the same. This is, in fact, the case in most compounds, and if the SLR rates are not very fast to cause thermalization, one should observe two types of EPR transitions between each pair of levels. One transition will be enhanced absorption (a) and the other an emission (e). The corresponding kinetic curves will also show enhanced absorption and emission transients superimposed on relatively slow components. This effect, known as electron spin polarization (ESP), can be observed by EPR on randomly oriented photoexcited triplets.[50] Two basic experiments, which are complementary to each other, are normally performed.[27]

(a) Direct display of the 100-kHz field modulated susceptibility, $d\chi''/dH$, at a particular field as a function of time. This type of experiment is performed when the sample in the EPR cavity is subjected to a train of square-wave light pulses, and the unfiltered signal output is fed into an averaging device. It is important that the rise and decay time of the light pulses will be shorter than the response time of the EPR spectrometer, which for most conventional spectrometers is determined by the field modulation frequency (~100 μs).

(b) Displaying $d\chi''/dH$ at a particular light excitation frequency and phase, as a function of the external magnetic field. This experiment is carried out when the light-dependent signal $d\chi''/dH$ is phase-sensitive detected (using an external phase-sensitive detector) with respect to the light modulation frequency. Typical examples of employing these two experiments are shown in Figure 4.

To analyze quantitively data acquired using light modulation, one should solve explicitly a set of four coupled differential equations which describe population A, depopulation k of the triplet sublevels, and SLR connecting each pair of levels.[51-54] An analytical solution is attainable only under some simplifying requirements such as (i) nonlight-saturating conditions, (ii) validity of eq 20, and (iii) certain restrictions on the SLR rates, W, among the triplet sublevels. For many porphyrins and chlorophylls (in vitro and in vivo), the first two requirements are easily fulfilled. It is difficult, however, to fulfill experimentally the third requirement if the measurements are performed at high temperatures. Such an approximation therefore results in small alteration in the kinetic parameters evaluated from the experimental curves. These difficulties can be avoided altogether by employing the analysis of the triplet dynamics using an analog computer as first proposed by Weissman.[55,56]

The ESP patterns in the triplet spectra using light modulation–EPR experiments warrant some additional remarks. In the fast light modulation frequency limit $\omega_L \gg 1/\tau$ (where ω_L is the light modulation frequency and τ is the total triplet lifetime), the polarized triplet spectrum is an image of the fast (transient) components in the triplet dynamics. Such a spectrum is shown by the lower trace of Figure 4. The directions of $d\chi''(\omega_L)/dH$ in the first harmonic representation at each canonical orientation indicate whether the transient is absorption (a) or emission (e). This is determined by the ISC rates governed by the spin–orbit interaction Hamiltonian (eq 13). Thus, a transient triplet spectrum in the fast limit will show one of six patterns. As an illustration the directions of the transitions in the $\Delta M_s = \pm 1$ region, as given by the lower trace of Figure 4, are e($2z$) a($1x$) e($1y$) a($2y$) e($2x$) a($1z$), where e and a are emission and absorption lines, respectively.[27] Notice that under the usual spin–orbit ISC mechanism as described earlier there is always a change in the sign

TABLE I. Kinetic Rate Parameters (in units of s^{-1}) and ZFS Parameters (in units of cm^{-1}) for Some in Vitro Compounds

Molecule	Solvent	T, K	k_x[a]	k_y[a]	k_z[a]	A_x[a]	A_y[a]	A_z[a]	$\|D\|$[a,b]	$\|E\|$[a,b]	Ref and method
Chl a	Pyr:Tol	~5							+0.0273	−0.0040	67 EPR
	n-Octane	85	800	1200	360	0.9	1.0	0.2	0.0262	0.0022	64 EPR
	n-Octane	2	661	1255	241	0.3	1.0	1.0	0.0280	0.0038	63 ODMR
	EtOH	95	710	2710	370	0.38	1.0	0.15			63 EPR
Chl b	Pyr:Tol	~5							+0.0293	−0.0052	67 EPR
	n-Octane	85	320	550	40	1.0	0.6	0.1	0.0286	0.0037	64 EPR
	n-Octane	2	268	570	34	0.3	1.0	0	0.0320	0.0041	63 ODMR
	EtOH	95	310	850	65	0.4	1.0	0.1			63 EPR
Chl c_1		~5							0.0269	0.0055	58 EPR
Chl c_2		~5							0.0276	0.0050	58 EPR
Ph a	Pyr:Tol	~5							+0.0342	−0.0033	67 EPR
	MeTHF	103	1040	1300	820	0.7	1	0.6	0.0341	0.0033	63 EPR
Ph b	Pyr:Tol	~5							+0.0347	−0.0038	67 EPR
	MeTHF	103	590	870	420	0.6	1	0.5	0.0358	0.0046	63 EPR
Bchl a	Pyr:Tol	~5							+0.0224	−0.0053	67 EPR
Bchl a	THF	2	2287	3321	661				0.0238	0.0069	65 ODMR
Bchl B	Pyr:Tol	~5							+0.0212	+0.0055	67 EPR
Bph a	Pyr:Tol	~5							+0.0259	+0.0046	67 EPR
Bph b	Pyr:Tol	~5							+0.0249	+0.0050	67 EPR
H_2TPP	*n*-Octane	80	300	600	150	0.31	0.54	0.14			
H_2P	*n*-Octane	4.2	75	230	6	0.31	0.68	0.01	0.0435	0.0063	32,38 ODMR
TPC	Tol:EtOH (5:1)	77	400	700	240	0.56	1.0	0.40	0.0364	0.0063	66 EPR
	n-Octane	105	500	900	250	0.6	1.0	0.36	0.0364	0.0063	66 EPR
MgTPP	Tol:EtOH (2:1)	100	Av decay rate 21[c]						0.0310	~0	66 EPR
	n-Octane	100	Av decay rate 15[c]						0.0310	~0	66 EPR
	EtOH	100	Av decay rate 48[c]						0.0310	~0	66 EPR
MgTBP	Tol:Pyr	5	Av decay rate 4.3[c]						0.0334	0.0065	63 EPR
ZnP	*n*-Octane	1.2	4.9	5.9	9.0	0.03	>0.04	0.93	0.035	0.009[d]	62 ODMR
ZnChl a	*n*-Octane	2	346	330	660				0.0306	0.0042	64 ODMR
ZnChl b	*n*-Octane	2	122	250	622	0.3	0.7	1.0	0.0328	0.0032	64 ODMR

[a] Coordinate systems are chosen such that *x*, *y* are in the molecular plane and *z* is out of plane. The order of the *X*, *Y*, *Z* energy levels are $X > Y > Z$. For experimental errors see appropriate references. [b] The sign in front of the ZFS parameter indicates that it has been determined uniquely. Those values without a sign indicate the absolute value. [c] These decay rate correspond to the total triplet lifetimes. [d] At 77 K in EPA glass; the same authors report $|E| \approx 0$.

(from e to a or vice versa) for a given set of transitions as defined by pi (cf. Figures 2 and 3). In those cases where no change in sign of polarization occurs, e.g., some photosynthetic pigments in vivo,[57-59] the above spin–orbit mechanism cannot account for the observations. For example, the experimentally observed[59] pattern of the type a(2*z*) e(1*x*) e(1*y*) a(2*y*) a(2*x*) e(2*y*) implies that, regardless of the direction of the magnetic field, it is always the T_0 (or alternatively the $T_{\pm 1}$) spin sublevels which are populated selectively. This observation and its structural implication will be discussed in section IV.

5. Optical NMR Experiments

The technique of in situ light excitation combined with NMR detection[60] has been recently pursued by Boxer and Closs[28] to problems in PS. The technique requires light excitation of the sample in the NMR probe. As triplet states are produced the following energy transfer reaction take place

$$C(T_1) + C(S_0) \rightleftarrows C(S_0) + C(T_1) \qquad (21)$$

where C is some chromophore. Since $[C(T_1)] \ll [C(S_0)]$, the NMR detects only the diamagnetic species $C(S_0)$. But on the average each chromophore molecule is momentarily perturbed by a paramagnetic triplet excitation which disturbs the precession of the nuclear spins. This frequent albeit short disruption of nuclear precession rates leads to NMR line broadening. The greater the line broadening of a particular NMR active nucleus for a given ratio $[C(C_0)]/[C(T_1)]$, the greater the spin density at the nucleus. Thus, this technique may provide an accurate means for mapping unpaired electrons in triplet molecules. This technique has two major drawbacks: (1) the absolute determination of a spin density depends on measuring simultaneously the NMR spectrum and the ratio $[C(S_0)]/[C(T_1)]$; (2) the high-resolution technique cannot be applied to in vivo PS systems where only broad lineups are observed in the NMR spectrum. A sufficiently accurate and direct measurement of $[C(T_1)]$ in the NMR probe is most difficult and not practical. However, relative spin densities are easily measured by this NMR technique. If one or two spin densities of the triplet state of interest are known from other techniques, (i.e., pulsed EPR and ENDOR methods), the problem of absolute spin densities is solved. Nevertheless, this technique promises to be of great value in the study of PS and triplets.

III. Triplet State Properties in Model Compounds

The basic skeleton of the chlorophylls is the porphyrin-like ring system.[61] It is expected, therefore, that the extensive research carried out on porphyrins and chlorophylls in vitro can be applied to intact cells of the photosynthetic apparatus. The model compounds which consist of free base and substituted porphyrins as well as various types of chlorophylls in vitro have been investigated using the techniques described in the previous sections.[32,58,59,62-67] Table I summarizes the optical, magnetic, and kinetic parameters of some porphyrins and chlorophylls in vitro in different environments and aggregate forms. Since many porphyrins and practically most chlorophylls are nonphosphorescing, application of ODMR has been restricted to fluorescence detection and triplet–triplet absorption detection.

Inspection of Table I shows that the ZFS parameters remain effectively the same in a particular series of compounds. The relatively small values of $|D|$ as compared to those reported for aromatic systems, $|D| \approx 0.1\ cm^{-1}$, $|E| \approx 0.014\ cm^{-1}$ for naphthalene,[68] is expected because of molecular dimensions and delocalization to a larger extent of the triplet excitation in the porphyrin-like compounds. Knowing the sign of the ZFS

parameters of in vivo chlorophylls is important for the determination of the structures and mechanisms which are involved in the primary events of PS. Since the optical properties of chlorophylls in vitro are known to a large extent both theoretically and experimentally, the MPS method has been applied to some of the Chl molecules.[67] Thus, the ordering of the ZFS energy levels *X, Y, Z,* i.e., the signs of *D* and *E*, has been determined by the application of the MPS method (cf. Table I). The application of the MPS method to in vivo chlorophylls are of interest and may be promising.[69]

Except for magnesium tetraphenyl and tetrabenzoporphyrin (MgTPP) and (MgTBP), respectively, all the model compounds listed in Table I exhibit an electron spin-polarized triplet state (ESP); i.e., the triplet sublevels are coupled selectively to the singlet manifold. All the different types of experiments indicate that essentially one spin component is the most active with respect to the population and depopulation rate constants.

In porphyrin or Chl compounds one generally defines the molecular coordinate system x, y, z such that the *z* component is perpendicular to the molecular frame. Also, it is assumed that the dipolar splitting is maximum along the *z* principal axis.[70,71] Thus, except for the zinc porphyrins or zinc chlorophylls, the results for most of the compounds, given in Table I, show that the active spin component lies in the molecular frame, namely T_x or T_y. In the zinc compounds the general phenomenon is that the out-of-plane component, T_z, is the most active one.[63,64] This difference in the kinetic rates has been interpreted qualitatively[64] using the interpretive approach of Metz et al.[72] developed in their studies of aromatic molecules. Clarke et al.[64] demonstrated that in planar aromatic compounds possessing a $\pi\pi^*$ triplet character, the in-plane components are the most active.[73] Thus, from this point of view incorporating the magnesium cation into the chlorin-type macrocycle does not affect to a large extent the $\pi\pi^*$ character of the system. In other words, the spin–orbit coupling which serves as a mechanism for ISC is not greatly affected by the light magnesium cation. On the other hand, the heavier zinc atom does affect the spin–orbit coupling via mixing of the d orbitals with the π system resulting in the out-of-plane axis as most active.[64] These studies suggest that the magnesium is of minor importance in affecting the triplet dynamics of the chlorophylls in vitro.[64] Nissani et al.[66] studied the triplet dynamics of MgTPP and tetraphenylchlorin (TPC) and compared the results to Chl in vitro. They found that the triplet dynamics of TPC are very close to those of Chl (in particular, Chl b), from which they derived the same conclusion reported by Clarke et al.[64] Bowman[74] investigated by optical techniques the triplet lifetimes of normal and fully deuterated Chl in dry and wet pyridine. He concluded that the ISC mechanism in the Chl molecule is achieved via a static distortion in which the central magnesium atom is forced in or out of the molecular plane by magnesium–solvent interaction. In Ph molecules he proposed a dynamic model in which ISC is achieved by out-of-plane N–H vibrations. Regarding the ESP patterns in the model compounds, the direction of polarization for each line intensity (the canonical orientations) in the EPR spectra is in accord with the mechanism of spin–orbit ISC coupling which generate the selective ISC rates (section II).

A different experimental and theoretical approach, using model compounds, is based upon current theories and experiments which have been reported for intact preparations. For example, it is accepted that the primary stage in PS involves a charge separation process. This implies photoreduction and photooxidation processes in the special pair apparatus. In other words, the charge separation in the reaction center involves an electron-transfer process. This raises the important question whether the photoelectron transfer involves an excited singlet or an excited triplet as a precursor.[5] A few studies have been reported on the photoreduction of porphyrins and porphyrin-like molecules.[75–77] Of particular interest is Bph which is considered to be part of the RC.[7–9] Gouterman and collaborators have investigated the electron transfer reaction from Bph to *p*-benzoquinone.[76,77] In this model system they demonstrated that the excited triplet of Bph reacts with the quinone to form the separate anion radicals $Bph^{\cdot+}$ and $Q^{\cdot-}$. They propose a charge separation mechanism via a charge transfer complex having a triplet character $\{Bph^{\cdot+}\ quinone^{\cdot-}\}^T$. These results are of importance and helpful in order to interpret some of the photoelectron transfer processes of the RC.

IV. In Vivo Triplets

A. Historical Background

After the pioneering suggestions of Franck and Rosenberg,[78] the major impetus for experimental observation of triplet states in photosynthetic organisms and pigments is mostly due to the work of Dutton, Leigh, and co-workers.[79–83] These workers observed an intense, highly polarized EPR triplet spectrum in photosynthetic bacteria. First they noted that the ZFS parameters were too small to be explained by a Bchl monomer, and thus they interpreted the ESP signal as arising from a triplet radical pair within the Bchl special pair, i.e., $Bchl^{\cdot+}Bchl^{\cdot-}$. Second they suggested that the unusual ESP patterns could be explained if an excess population of the T_0 spin sublevel existed for all canonical orientations. Finally they demonstrated that the triplet state observed by EPR was associated with the blocking of the primary electron acceptor pathway, presumably at the quinone–iron complex (cf. eq 5, section I). More recent work suggested that the unusual ESP patterns result from a radical pair (RP) intermediate consisting of oxidized special pair and the preprimary electron acceptor (probably Bph), i.e., $[(Bchl)_2^{\cdot+}\text{-}Bph^{\cdot-}]$.[7–9,59] Unlike bacteria, the triplet state observed in algae did not appear to arise in the reaction center.[57,66] Furthermore, the algae exhibited monomeric ZFS parameters and "normal" ESP patterns. Furthermore, these early investigations clearly demonstrated, particularly in bacteria, that the triplet state probably originated in the Bchl special pair and was structurally and mechanistically important.

We shall now explore in more detail the significance of these in vivo triplet state observations and offer current interpretations of the origin and mechanism of triplet formation in photosynthetic organisms.

B. Triplet State in Bacterial Photosynthesis

1. Origin of the Triplet State

In order to observe an intense triplet signal it is necessary to reduce the quinone species prior to the photoexcitation. Much weaker signals are observed otherwise. One important exception to this observation has been reported by Okamura et al.[84] who observed large triplet signals in R-26 RC that contains no quinone. This result is not, however, in conflict with the prior reduction scheme since in this case the absence of quinone is equivalent to the reduction of quinone. In both cases, the electron flow is stopped at the preprimary electron acceptor. Since R-26 RC also contains no carotenoids, the only remaining reasonable species for the origin of the triplet state is either Bchl or Bph.

In the RC two molecules of Bchl absorb at ~800 nm (P_{800}), two at ~870 nm (P_{870} special pair), and two Bph molecules at ~760 nm. As yet no direct measurement of $T_1 \rightarrow S_0$ transition has been reported for either Bchl or Bph. However, very weak $T_1 \rightarrow S_0$ phosphorescence has been observed[85,86] for Chl a, Chl b, Ph a, and Ph b. It is perhaps relevant that the triplet–singlet energy gap is found to be related to the singlet–singlet energy gap in monomers via the empirical relation $\Delta E_{T_1 \rightarrow S_0} \approx k\Delta E_{S_1 \rightarrow S_0}$. Most determinations place *k* at approximately 0.7 implying that the triplet state of Bph lies above that of Bchl special pair P_{870} by ~1000 cm^{-1}, or by ~170 cm^{-1} if one employs $\Delta E_{S_1 \rightarrow S_0}$ for the monomer Bchl. Such a situation has been confirmed by Gouterman and Holten[77] and also in vitro experiments by Boxer and Closs using the optical–NMR tech-

TABLE II. Kinetic Rate Parameters (in units of s^{-1}) and ZFS Parameters (in units of cm^{-1}) for Some in Vivo Preparations

Species	T, K	k_x[a]	k_y[a]	k_z[a]	A_x[a]	A_y[a]	A_z[a]	$\|D\|$[a,b]	$\|E\|$[a,b]	Ref and method
					In Vivo Bacteria					
^{1}H-*R. rubrum*	4.8–9							+0.0185[c]	0.0033	67 EPR
^{2}H-*R. rubrum*	4.8–9							0.0185	0.0034	67 EPR
^{1}H-*Rps. spheroides*	4–9							0.0182	0.0035	67 EPR
^{2}H-*Rps. spheroides*	4–9							0.0183	0.0032	67 EPR
^{1}H-*Rps. palustris*	4–9							0.00182	0.0035	67 EPR
^{2}H-*Rps. palustris*	4–9							0.0184	0.0031	67 EPR
^{1}H-*Rps. gelatinosa*	4–9							0.0184	0.0028	67 EPR
^{1}H-*Rps. spheroides*	4–9							0.0183	0.0031	89 EPR
^{1}H-*Rps. spheroides* Ga	4–9							0.0185	0.0031	89 EPR
^{1}H-*R. rubrum* G9	4–9							0.0185	0.0031	89 EPR
^{1}H-*Chromatium* D	4–9							0.0178	0.0033	89 EPR
^{1}H-*Rps. spheroides* Ga	4–9							0.0185	0.0031	89 EPR
^{1}H-*Rps. gelatinosa*	4–9							0.0186	0.0027	89 EPR
^{1}H-*Rps. spheroides* R-26	4–9							0.0186	0.0031	89 EPR
R. spheroides (wild type)	1.8	9300	8500	2100	0.437	0.449	0.094	0.01872	0.00312	90 ODMR
R. spheroides R-26	1.8	9000	8000	1400	0.484	0.445	0.071	0.01878	0.00322	90 ODMR
R. rubrum	1.8	9000	8000	1400	0.488	0.437	0.0075	0.0190	0.0034	90 ODMR
R. rubrum	1.8	2105	2885	1335				0.0190	0.0034	91, 92 ODMR
R. spheroides R-26	1.8	2660	3183	1596				0.0188	0.0031	92 ODMR
R. spheroides (2.4.1)	1.8	2674	3033	1600				0.0189	0.0032	92 ODMR
Chromatium vinosum Strain D	1.8							0.0181	0.0034	92 ODMR
					In Vivo Green Plants					
Anacystis nidulans										
A	4.2							0.0283	0.0038	93 ODMR
B	4.2							0.0348	0.0021	95 ODMR
C	4.2							0.0311	0.0038	93 ODMR
D	4.2							0.0366	0.0020	93 ODMR
Porphyridium cruentum	4.2							0.0283	0.0037	93 ODMR
Euglena gracilis	4.2							0.0297	0.0037	93 ODMR
Chlorella A	4.2							0.0288	0.0038	93 ODMR
Chlorella C	4.2							0.0311	0.0038	93 ODMR
Chlamydonomas reinhardi 35		850 500	1300 560	320 60	0.7 0.6	1:0	0.2 0.1	0.0280	0.0032	66 EPR
Spinach chloroplasts	4.5							0.0284	0.0039	57 EPR

[a] See footnote *a* of Table I. [b] See footnote *b* of Table I. [c] For sign determination see ref 94 and 95.

nique.[87] More direct observations are those reported by Parson et al.[88] on photosynthetic bacterial RC. In a laser photolysis experiment they monitored a transient absorption attributed to a triplet–triplet transition. This new absorption was similar to the triplet–triplet absorption in monomeric Bchl (or Bph) and has a lifetime of submilliseconds. As long as this triplet–triplet transition was observed, P_{870} demonstrated bleaching. The P_{800} peak was affected only slightly, probably in the form of a shift. A small change in P_{800} is expected owing to its close proximity to the special pair implying that $S_1 \leftarrow S_0$ in P_{800} is slightly coupled to the corresponding transition in P_{870}. This interpretation is supported by the spectroscopic changes that take place when P_{870} is oxidized to form the cation radical.[88] In this case P_{870} is completely bleached and P_{800} in the RC is slightly shifted. As regards Bph, it should be indicated that small changes in its absorption spectrum occur also. Thus, according to all evidence the most likely origin of the observed triplet is mostly the $(Bchl)_2$ special pair. Nevertheless, it should be emphasized that none of these experiments eliminate rigorously the participation to some extent of Bph or P_{800} in the triplet state and more direct observations (which are extremely difficult) are in order. We thus take the approach of explaining the triplet state ZFS of bacteria by primarily considering Bchl special pairs that absorb near 870 nm.

2. Zero-Field Splitting Parameters

The ZFS parameters have been determined for a number of photosynthetic bacteria. Table II is a selective summary of such data which we believe represents the best recent values. It is evident that the $|D|$ and $|E|$ values obtained for all bacteria are noticeably smaller than those of the corresponding monomeric species given in Table I. The reduction in $|D|$ indicates that the triplet is delocalized over more than a single molecule of Bchl, probably the $(Bchl)_2$ special pair. The occurrence of a relatively large $|E|$ indicates a significant deviation from axial symmetry.

How does the reduction in $|D|$ occur? Solvent or environmental effects are generally small, particularly for $|D|$, and thus cannot be invoked here. The two remaining mechanisms are the following: (a) a formation of a radical pair (RP) such as $Bchl^{\cdot+}Bchl^{\cdot-}$ or $(Bchl)_2^{\cdot+}Bph^{\cdot-}$, and (b) triplet migration through an aggregate, in particular, $Bchl^{T_1}Bchl^{S_0} \rightleftarrows Bchl^{S_0}Bchl^{T_1}$.

In a RP of mechanism a such as $Bchl^{\cdot+}Bchl^{\cdot-}$, one expects to observe a triplet EPR spectrum with characteristic $|D|$ and $|E|$ values. In general, both $|D|$ and $|E|$ are small for radical pairs since one unpaired triplet electron is on one molecule ($Bchl^{\cdot+}$) and the other unpaired electron is on another molecule ($Bchl^{\cdot-}$). Hence the dipole–dipole interaction responsible for the ZFS should be small. How small should the ZFS be for $Bchl^{\cdot+}Bchl^{\cdot-}$? In order to answer this question one must proceed by making a comparison with the triplet state of monomeric Bchl. On monomeric Bchl the two triplet electrons are always confined within the molecular framework and necessarily are expected much closer together on the average than are the two electrons in $Bchl^{\cdot+}Bchl^{\cdot-}$. Thus one expects, because of the inverse cube effect (eq 10), that the ZFS of $Bchl^{\cdot+}Bchl^{\cdot-}$ would be very much smaller than the ZFS of monomeric Bchl triplets. Since the ob-

served reduction (cf. *R. Rubrum* vs. Bchl monomer) is not very large (~20% reduced), the pure RP explanation for the smaller ZFS in *R. Rubrum* is not considered very likely. Thus we are left with mechanism b in order to account for the fairly small reduction of the ZFS parameters as observed. Actually both mechanisms may operate simultaneously, but in the case of bacteria, mechanism b seems to dominate in reduction of $|D|$. It is noteworthy to add that the above arguments are not conclusive in the elimination of a RP mechanism. One can easily visualize a RP in which the macrocycle planes are stacked on top of each other with a very short electron–electron distance between almost all sites. This requires an end-to-end dipolar interaction [→→] rather than a side-by-side dipolar interaction [↑↑]. The former interaction requires $D < 0$ (Figure 2), whereas the latter is found in most planar aromatics where $D > 0$.[96] Norris and Thurnauer[94,95] have determined that $D > 0$ in *R. Rubrum* and thus have eliminated the pure RP as an explanation for the reduced ZFS in the in vivo triplet state observed in bacteria. We reemphasize that this does not mean that the observed triplet is not preceded by a radical pair such as $(Bchl)_2^{\cdot+}Bph^{\cdot-}$ which is responsible for the ESP observed in $(Bchl)_2$.

The pure mechanism b increases the delocalization of the pair of triplet electrons via the migration and thereby may reduce the ZFS. In contrast to mechanism a, both electrons are always on the same molecule, and thus the electron–electron distances are not reduced. How then does one visualize the reduction in ZFS? As we have previously pointed out not only do $|D|$ and $|E|$ depend on the molecular dimensions, i.e., electron–electron separation distances, but they depend on the *"magnetic"* symmetry of the aggregate. Thus if the dimer structure moves to higher symmetry, then the ZFS become smaller (cf. section II). In the monomer, suppose that x and y are in the plane of the macrocycle with z normal to the plane and that the canonical orientation along z gives the largest dipolar splitting. Then by mechanism b, as long as the two z axes are parallel, $|D|$ will not decrease. If the two z axes are parallel and one molecule has been rotated by 90° about its z axis, then $|E|$ vanishes even though $|D|$ remains the same. Of course, the "hopping" rate of "delocalization" must exceed at least by roughly an order of magnitude the difference in dipolar energy X and Y. In other words, the dimer has a magnetic axial symmetry and x and y of the aggregate are indistinguishable magnetically. In this case $|E|$ has been reduced by an increase in the symmetry of the dipole–dipole interaction via aggregation. In order to decrease $|D|$ by mechanism b alone, the z axes cannot be parallel.

We hasten to add that if all canonical orientations of the two molecules are lined up in the special pair (0 to 180° rotation about any axis in one member of the pair), no reduction of the ZFS splittings will be observed for mechanism b. This situation can be detected by measuring the hyperfine interaction of the triplet state of the dimer. If the "hopping" rate is faster than the hyperfine interaction energy, then the triplet will be associated with twice the number of nuclei as found in the monomeric triplet. Unfortunately hyperfine interaction in triplets is difficult to measure. Again, the optical–NMR technique appears the most promising to measure hyperfine interaction in triplets observed in vitro.

3. *Electron Spin Polarization and the Radical Pair–Intersystem Crossing Mechanism*

In photosynthetic bacteria the ESP pattern is a(2z) e(1x) e(1y) a(2y) a(2x) e(1z).[59] This pattern can be observed if for $D > 0$ the center level T_0 is overpopulated relative to the upper and lower levels $T_{\pm 1}$. Although we have rejected a pure radical-pair explanation as the origin of the smaller in vivo ZFS, we would like to consider a RP–ISC mechanism for the ESP pattern observed in bacteria.

Let us assume that the three populations of the spin sublevels at zero magnetic field are N_{T_i}, $i = x, y, z$. The nine corresponding populations at high magnetic field, neglecting SLR processes, are given (to first order):[31]

$$N_{T_{01}} = N_{T_{i1}} \qquad i \| H \quad i = x, y, z$$
$$N_{T_{\pm 11}} = \tfrac{1}{2}(N_{T_{j1}} + N_{T_{k1}}) \tag{22}$$

Equation 22 is based on the usual spin–orbit ISC described in section II. The ESP pattern in bacteria requires that T_0 be overpopulated for all canonical orientations, namely

$$N_{T_{01}} = N_{T_{i1}} > N_{T_{\pm 11}} \qquad i \| H \quad i = x, y, z \tag{23}$$

It is easy to show that eq 23 leads to the inequality

$$\sum_i N_{T_{i1}} > \tfrac{1}{2}\left(2 \sum_i N_{T_{i1}}\right) \qquad i = x, y, z \tag{24}$$

which is clearly impossible. Thus, ordinary ISC will never produce overpopulation of T_0 at all high-field canonical orientations. Variations of the ordinary ISC that include SLR still are not capable of accounting for the observed high-field EPR spectra.

The simplest explanation for overpopulation of only T_0 for all high-field canonical orientation is via the so-called RP mechanism. This mechanism has been discussed extensively in the so-called phenomena of chemically induced dynamic nuclear[97] or electron[98] polarization CIDNP or CIDEP, respectively. For example, consider the reactions (eq 25) that results in the special

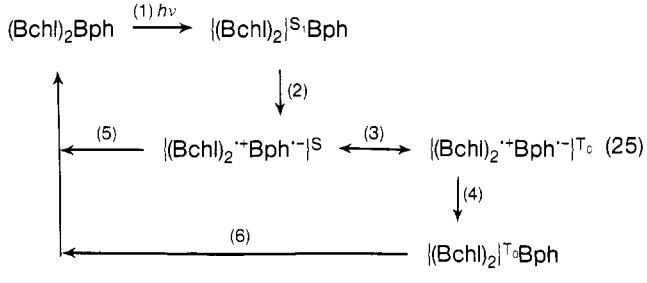

(25)

pair triplet. Prior to process 2, the electrons are correlated as a singlet state and thus the initial electron transfer produces a singlet state. Because of the large distance between the electrons in the radical pair, the correlation begins to change owing to different Larmor frequencies of the electron spins on $(Bchl)_2^{\cdot+}$ and $Bph^{\cdot-}$. Hence, this dephasing process causes the spin angular momentum of the electron pair to change back and forth from $M_{S=0} = 0$, S, to $M_{S=1} = 0$, T_0. The difference in magnetic environment may be provided by hyperfine interaction, g-factor differences, or interaction of either spin with other paramagnetic species in the RC. Conversion of singlet radical pair to the $T_{\pm 1}$ radical pair is also possible, but as long as the electrons are sufficiently separated, this type of mixing is negligible. Once the triplet character is developed a back electron transfer produces an ordinary triplet (process 4). Processes 5 and 6 result in the ground-state singlet.

We summarize the mechanism that seems to fit most observations about the triplet state in bacteria PS in Figure 5. Notice that observation of the triplet is possible only in the blocked mechanism (B) where the acceptor Q–Fe has been reduced. The observed EPR triplet is basically *an ordinary* delocalized triplet, which is produced by process 4, and decays by the usual ISC mechanism. The unusual feature of this state is in its birth which is via a RP–ISC mechanism. This triplet state is commonly referred to as P^R.[88] Notice that the P^F state which is a triplet radical pair is not observed owing to its very short lifetime on the EPR time scale.[6,7] When the system is unblocked (U), the 250 ps for process 3 does not allow the conversion of a significant amount of singlet radical pair into triplet radical pair. Instead, a new radical pair is formed via process 3. However, if the state produced via process 3 were to back-react directly, not enough energy is present to reach the $(Bchl)_2$ in the T_0 state, and instead $(Bchl)_2$ in the ground state is formed. Back reaction of this state

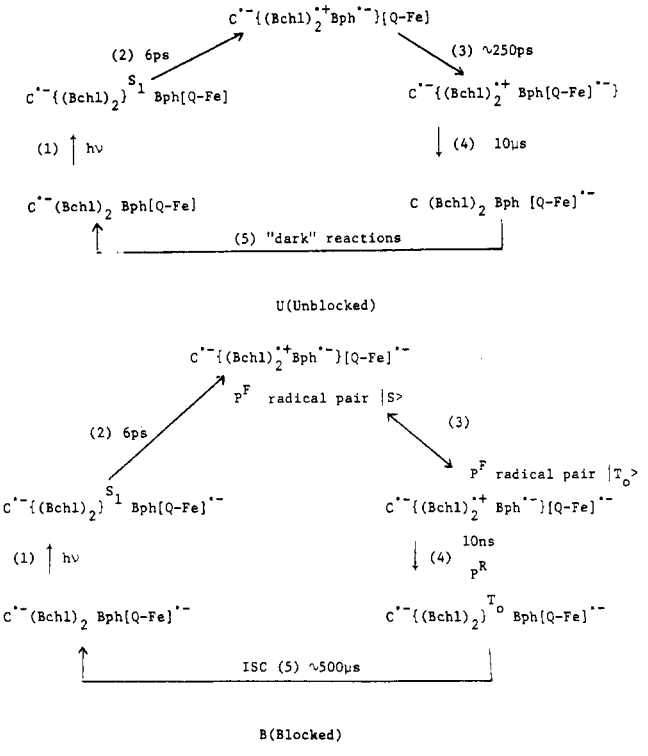

Figure 5. "Blocked" (B) and "unblocked" (U) reactions in the bacterial photosynthetic reaction center. A singlet state which is indicated without an index, i.e., S, is due to a radical pair singlet configuration. The term C corresponds to cyctochrome.

is generally avoided in the natural course of events by a fast microsecond reaction of reduced cytochrome with the cation special pair.[14] Schemes U and B represent the most frequently encountered explanation of the primary events in bacteria and the role of the triplet state. The reaction times of U and B represent either optical data or magnetic resonance lifetimes. The radical pair state as shown in Figure 5 employs $(Bchl)_2$ and Bph. The magnetic resonance data can directly detect only the P^R state, and thus invokes a radical pair precursor via indirect means. Any radical pair with sufficiently fast conversion into T_0 is sufficient to explain the triplet ESP pattern of bacteria.[99]

The most direct evidence on the chemical nature of the radical pair state P^F is from fast time-resolved optical studies.[6-9,88] The optical transient associated with this state agrees best with $(Bchl)_2^{\cdot+}Bph^{\cdot-}$. The spectral changes occur within ~6 ps and last for ~250 ps in an unblocked system (Figure 5U) and ~10–30 ns in a blocked system (Figure 5B).[88] The observed spectral differences include bleaching of P_{870} with a corresponding increase at 1250 nm where P_{870}^{+} absorbs.[9] Also bleaching occurs near 540 nm where Bph absorbs.[9] Thus, the state P^F has tentatively been identified by some authors as a $(Bchl)_2^{\cdot+}Bph^{\cdot-}$ radical pair.[5,8,100]

In the mechanism of Figure 5 (U and B) the triplet state is not on the essential photosynthetic pathway. The radical pair state P^F of the primary charge separation occurs from a singlet state. Moreover, in most of the in vivo experiments, the corresponding reactions indicate the involvement of the photoexcited singlet in electron reactions.[5,21,76,77] Fong,[101] however, has proposed a charge transfer in the Bchl special pair that requires a triplet state on the essential pathway. We present Fong's scheme in Figure 6. This scheme requires that the charge-transfer state of the special pair is initially in a triplet state which is formed by the most usual ISC mechanism. Thus in Fong's model the RP state that gives rise to the observed triplet when quinone is blocked starts out in a triplet state where all three spin sublevels $T_{\pm1}$ and T_0, must be populated. At this point this mechanism would not be able to explain the ESP pattern observed in bacteria. Additional ESP will develop in the radical pair when

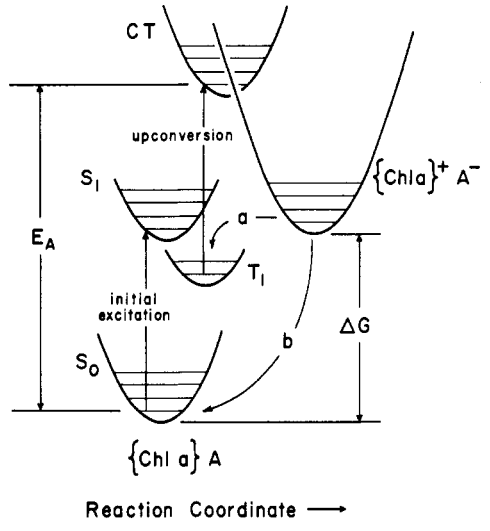

Figure 6. Schematic representation of Fong's model involving the triplet precursor prior to the charge separation (taken with permission from ref 101).

$$\{(Bchl)_2^{\cdot+}Bph^{\cdot-}\}^{T_0} \underset{RP}{\overset{ISC}{\rightleftarrows}} \{(Bchl)_2^{\cdot+}Bph^{\cdot-}\}^{S} \rightarrow \{(Bchl)_2\}^{S_0}Bph \quad (26)$$

In this case T_0 of the radical pair P^F would be depleted, thus giving a polarization pattern (in the P^R state) e(2z) a(1x) a(1y) e(2y) e(2x) a(1z) which is exactly opposite to the observed a(2z) e(1x) e(1y) e(2z) a(2x) e(1z). The above mechanisms are compared schematically by eq 27 and 28. The former process is

$$|S_0> \longrightarrow |S_1> \longrightarrow |S>_PF \xrightarrow{RP\text{-}ISC} |T_0>_PF \longrightarrow |T_0>_PR \xrightarrow{SO\text{-}ISC} |S_0> \quad (27)$$

$$|S_0> \longrightarrow |S_1> \xrightarrow{SO\text{-}ISC} |T_1> \longrightarrow |T_{CT}> \longrightarrow |T_0>,|T_{+1}>|_PF \longrightarrow |T_0>, \longrightarrow |T_{+1}>|_PR, \quad (28)$$

RP-ISC: $|S>_PF$; SO-ISC: $|S_0>$

carried out via a singlet precursor, and the latter process is carried out via a triplet precursor.

Regardless of the nature of P^R,[102] i.e., its exact identity, the observed ESP pattern of bacteria is unexplained by the Fong mechanism. We emphasize that although this appears to be a problem for the Fong mechanism in bacteria, the situation in green plants may be different.

4. *Triplet Parameters and Structure of the Special Pair*

Since bacterial PS has been studied extensively, we shall describe in some length the recently proposed models for the special pair structure in bacterial PS as inferred from the triplet state.

In the previous sections we pointed out that in the ESP patterns, the magnitude and sign of the ZFS parameters may vary from one system to the other. The sensitive variations are normally interpreted in terms of inter- and intramolecular processes, thus providing a closer insight into the mechanism of charge separation and subsequent processes (triplet–RP or conventional triplets). We now describe how the magnetic and kinetic parameters of the photoexcited triplet state can be related to the structure of the RC special pair.

Several specific structures have been proposed for the special pair.[65,103-105] Some of them are based on the experimental data obtained for in vivo experiments. Other proposed structures are based on model compounds such as porphyrins and Chl in vitro whose general physical properties are known to a large extent. In the original model introduced by Katz et al.,[103] the two Chl molecules, which are parallel to one to the other, are held together by a single water molecule. On the basis of two equivalent Chl species held together by two water molecules, Fong[104] proposed a C_2 symmetry for the pair of Chl molecules, again with parallel macrocycles.[107] Clarke et al.[65] pointed out that two water molecules force the planes to remain parallel whereas one water molecule enables the macrocycle planes to deviate from a parallel configuration.

The decreases in ZFS parameter $|D|$ for in vivo triplets, as compared to in vitro Bchl, may be interpreted either partially by charge-transfer character in the special pair or by an out-of-plane tilt of the macrocycle planes relative to one another. Recently Shipman et al.[105] proposed a different special pair structure than originally suggested. The new structure has a C_2 symmetry where the two macrocycle planes remain parallel but are closer, ~3.5 Å. This allows for a more efficient charge separation, and thus a small contribution of about 15% of RP character is attributed to the overall triplet state observation. We previously mentioned that the triplet energy of Bchl is estimated at ~0.7 of the $\Delta E_{s_1 \leftarrow s_0}$ energy gap. In the case of P_{870}, this gap is 1.4 eV. On that basis the triplet energy is ~0.98 eV. The energy of formation of $(Bchl)_2^{\cdot+}Bph^{\cdot-}$ has been estimated to be ~1.0 eV.[5] Thus, on an energy basis, inclusion of a small charge-transfer contribution to the pair $(Bchl_2)^3Bph$ in the form of $(Bchl_2)^{\cdot+}Bph^{\cdot-}$ is not unreasonable. Clarke et al.[65] proposed a structure where the normals to the planes of the two macrocycles make an angle of 48°, and the in-plane axes of the two molecules are rotated about 78° relative to one another. In contrast to the above-mentioned model, these authors invoke no RP or charge-transfer character to account for their results. Their analysis is based upon interpreting both the ZFS and ISC rates observed in the RC special pair in terms of the theory of triplet state of interacting organic molecules in the triplet state.[106] At this point it would be noteworthy to add that contradictory interpretations as regards to the structure and relative orientations of the monomeric species in the dimer have been reported by Mar and Gingras[120] and by Shuvalov et al.[121] In dichroic experiments the former group concludes the existence of nonparallel dipoles in the special pair, whereas the latter concludes a parallel configuration.

It is obvious that no experimental and theoretical data have been provided yet to justify conclusively a particular model. The successful synthesis of covalently linked porphyrins[122-124] are of extreme importance in elucidating the mechanism and structure of the special pair in PS.

C. Triplet State in Green Plant Photosynthesis

In green-plant preparations, the study of triplet state is incomplete. The original report, of EPR detection of triplets in green plants, by Leigh and Dutton[81] has not been unambiguously reconfirmed. There are some reports on the direct EPR[57,66] and ODMR[93,108,109] detection of triplets in green plants. A common feature in all these reports is that the triplet production is small, and the computed ZFS parameters $|D|$ and $|E|$ are very close to those reported for monomeric species. Moreover, the polarization (ESP) patterns in the triplet EPR spectrum have normal behavior. Thus, it seems very likely that in these observations the triplet observations are due to antenna Chl, and the question arises as to what is the biological origin of these triplets.

Indirect observations regarding the triplet state have also appeared. Blankenship et al.[110] applied CIDEP techniques to green-plant PS. Treating chloroplasts, these authors invoked a triplet state on the essential pathway of photosystem I following the detection of a polarized doublet (emission) EPR spectrum, at room temperature, in the microsecond time domain. This type of mechanism is normally known as triplet mechanism (TM). More recently Sauer et al.[111] and Dismukes et al.[112] reported on experiments where the chloroplasts flow rate through the EPR cavity was changed. In these experiments they could observe both absorption and emission EPR lines (depending on the flow rate). Since a triplet precursor mechanism could not explain their latter observations, they withdrew the TM and invoked the RP mechanism. The suggested RP mechanism invoked by these authors is based upon different g values of the two radicals of the RP which were proposed to be the primary electron donor $P_{680}^{\cdot+}$ and the corresponding acceptor $A^{\cdot-}$. These authors suggest that the precursor for the pair of radicals is the photoexcited singlet state of P_{700}. McIntosh and Bolton[113] have investigated the doublet EPR spectra originating after light irradiation of green algae at freezing temperatures. The observed two EPR signals which were interpreted by the authors to be emissive, were attributed to the primary electron donor, $P_{680}^{\cdot+}$ and electron acceptor $A^{\cdot-}$ in photosystem II. Since the normal RP mechanism seems to be ruled out in this case,[114] the TM, i.e., triplet precursor, was invoked by the authors. Although TM at low temperature is more probable then the RP mechanism, the scarce experimental results (also on model compounds) prevent a conclusive determination of the mechanism for the polarization. In particular, this is true for low-temperature measurements for which the existing theories for CIDEP should be examined. Nevertheless, the application of CIDEP techniques to the study of PS is in its early stages and may be promising as a new tool for the study of PS and the role of the triplet state in PS.

V. Concluding Remarks

Most mechanisms for the primary act of PS implicitly or explicitly involve singlet excited chlorophyll and no triplet excited states of chlorophyll. RP states (which in part may be regarded as triplet states) formed in the primary electron flow are easily interpreted as arising from singlet excited Chl states. To the best of our knowledge, as yet, no convincing experimental evidence requires the participation of excited triplet states of Chl in the main stream of PS. On the contrary, we have advanced arguments in this review that suggest that the triplet state P^R observed in bacterial PS results from an undesirable "back" reaction of the electron flow. In this view the triplet state in bacteria is not on the main pathway. The RP mechanism for the formation of triplet P^R has received recent support from magnetic field studies of bacteria where absorption changes associated with P^R have been monitored as a function magnetic field. These workers concluded that the birth of P^R was explained by a radical-pair mechanism.[115,116] In that respect, it will be interesting to apply the technique of magnetic field dependence on the population of the triplet manifold via changes in fluorescence or triplet–triplet absorption.[117] That the observed triplet, P^R, is produced by the RP–ISC mechanism is supported also by studies which have chemically blocked the electron flow close to the primary donor Bchl special pair.[118] Thus, when the preprimary electron acceptor is blocked by photochemical reduction, the triplet P^R is no longer observed. In this view, since no electron transfer can occur to form a photoinduced RP, no subsequent triplet should be formed. Although much evidence exists in bacteria for the triplet state P^R being associated only with the backward electron flow, it is still true that much structural and mechanistic information will eventually be obtained from studies of the triplet state in bacteria.

In green plants the role of the triplet state is less clear. In general the triplet states which have been observed have been extremely dilute, and no clear relationship with the reaction center has been established. More promising are the CIDEP

studies which have implicated triplet or radical-pair mechanisms. Thus one of the most promising areas for future investigation of the role of the triplet state in PS is in the indirect technique of CIDEP. Of special interest will be studies that will determine the role of the triplet state in green-plant PS.

In this survey we have not discussed the possible mechanism of selective ISC via triplet–triplet fusion or singlet–singlet fission $T_1 + T_1 \rightarrow S_0 + S_1$ or $S_0 + S_1 \rightarrow T_1 + T_1$, respectively. For this mechanism to occur two triplet-state energies should be equivalent to one singlet-state energy. Except for one report which place $k = 0.5$[119] in the relation $\Delta E_{T_1 \rightarrow S_0} = k\Delta E_{S_1 \rightarrow S_0}$, most studies report a higher value for k. Nevertheless, more direct measurement of the triplet-state energy are of importance for settling this question.

VI. Glossary and Terms

$\|0\rangle$, $\|\pm1\rangle$	Triplet spin wave functions at high magnetic fields
AP	Antenna pigments
$A_i (i = x, y, z)$	Population rate constant (intersystem crossing rate) to a triplet state at zero external magnetic field
Bchl	Bacteriochlorophyll; for structure see ref 22
Bph	Bacteriopheophytin; for structure see ref 22
CIDEP	Chemically induced dynamic electron polarization
CIDNP	Chemically induced dynamic nuclear polarization
Chl	Chlorophyll; for structure see ref 61
ENDOR	Electron nuclear double resonance
EPR	Electron paramagnetic resonance
H_2TPP	Tetraphenylporphyrin; for structure see ref 61
ISC	Intersystem crossing
$k_i (i = x, y, z)$	Depopulation rate constant from a triplet spin substate to the ground singlet at zero external magnetic field
MgTBP	Magnesium tetrabenzoporphine; for structure see ref 61
MgTPP	Magnesium tetraphenylporphyrin; for structure see ref 61
MPS	Magnetophotoselection
ODMR	Optical detection of magnetic resonance
OEPR	Optical electron paramagnetic resonance
OMR	Optical magnetic resonance
ONMR	Optical nuclear magnetic resonance
P_λ	A term indicating the wavelength of the absorption spectrum of a pigment, employed most frequently in photosynthesis
P^F	A term indicating the fast transient which is involved with the charge separation in the special pair
P^R	A term indicating a transient that originates from P^F; this intermediate has a longer lifetime than P^F
PS	Photosynthesis
RC	Reaction center
RP	Radical pair
S	Spin operator
SO	Spin–orbit
SLR	Spin–lattice relaxation; the rate for this process is designated as W
TM	Triplet mechanism
T_0, $T_{\pm1}$	Spin substates of the first excited triplet state at high magnetic field ($g\beta H \gg D$)
$\|T_i\rangle$ $(i = x, y, z)$	Pure spin wave functions at zero external magnetic field
T_i $(i = x, y, z)$	Spin substates of the first excited triplet state at zero external magnetic field; in some cases, when it is necessary, we express this state explicitly at T_{i1} $(i = x, y, z)$
TPC	Tetraphenylchlorine; for structure see ref 61
ZFS	Zero-field splitting; it can be expressed either in terms of the triplet energy levels X, Y, Z or the proper combination D and E

Acknowledgments. We are indebted to our colleagues Dr. Marion Thurnauer and Dr. Larry Patterson for reading the manuscript and their helpful criticisms and suggestions. We thank many of our colleagues all over the world who updated us with their recent reports. One of us (H.L.) would like to express his thanks to his friends at the Radiation Laboratory, University of Notre Dame, for their very kind hospitality during his stay in the U.S.

VII. References and Notes

(1) C. B. Van Niel, "Photosynthesis of Bacteria", in contribution to Marine Biology, Stanford University Press, Palo Alto, Calif., 1930, p 6.
(2) C. B. Van Niel, *Bacteriol. Rev.*, **8**, 1 (1944).
(3) M. Calvin, *Photochem. Photobiol.*, **23**, 425 (1976).
(4) "Bioenergetics of Photosynthesis", Govindjee, Ed., Academic Press, New York, N.Y., 1975.
(5) For a recent review see R. K. Clayton in "The Photosynthetic Bacteria", R. K. Clayton and W. R. Sistrom, Ed., Plenum, New York, N.Y., 1977.
(6) K. J. Kaufmann, P. L. Dutton, T. L. Netzel, J. S. Leigh, and P. M. Rentzepis, *Science*, **188**, 1301 (1975).
(7) M. G. Rockley, M. W. Windsor, R. J. Cogdell, and W. W. Parson, *Proc. Natl. Acad. Sci. U.S.A.*, **72**, 2257 (1975).
(8) J. Fajer, D. C. Brune, M. S. Davis, A. Forman, and L. D. Spaulding, *Proc. Natl. Acad. Sci. U.S.A.*, **72**, 4916 (1975).
(9) P. L. Dutton, K. J. Kaufmann, B. Chance, and P. M. Rentzepis, *FEBS Lett.*, **60**, 275 (1975).
(10) J. R. Norris, R. A. Uphaus, H. L. Crespi, and J. J. Katz, *Proc. Natl. Acad. Sci. U.S.A.*, **68**, 625 (1971).
(11) J. R. Norris, M. E. Druyan, and J. J. Katz, *J. Am. Chem. Soc.*, **95**, 1680 (1973).
(12) G. Feher, A. J. Hoff, R. A. Isaacson, and J. D. McElroy, *Abstr. Biophys. Soc.*, **17**, 61a (1973).
(13) The [Q–Fe] complex is normally called the primary acceptor because of historical precedent.
(14) W. W. Parson, *Biochem. Biophys. Acta*, **131**, 154 (1967).
(15) G. Doring and H. T. Witt, *Proc. 3rd Int. Congr. Photosyn. Res., 1971*, 39 (1972).
(16) For a general textbook see, J. B. Birks, "Photophysics of Aromatic Molecules", Wiley-Interscience, New York, N.Y., 1970.
(17) For a general textbook and references see, S. D. McGlynn, J. Azumi, and M. Kinoshita, "Molecular Spectroscopy of the Triplet State", Prentice-Hall, Englewood Cliffs, N.J., 1969.
(18) D. L. Van der Meulen and Govindjee, *J. Sci. Ind. Res.*, **32**, 62 (1973).
(19) J. R. Norris, *Photochem. Photobiol.*, **23**, 449 (1976).
(20) J. R. Bolton and J. T. Warden in "Creation and Detection of the Excited State", Vol. 2, W. R. Ware, Ed., Marcel Dekker, New York, N.Y., 1974, p 63.
(21) P. A. Loach, *Photochem. Photobiol.*, **26**, 87 (1977).
(22) P. A. Loach in "Progress in Bioorganic Chemistry", Vol. 4, E. T. Kaiser, Ed., Wiley, New York, N.Y., 1976, p 90, and references therein.
(23) In PS studies introduced first by L. N. Duysens, Ph.D. Thesis, Utrecht, 1952.
(24) For an extended list of references regarding the application of these experimental techniques, see ref 5 and 21 in this review.
(25) G. E. Busch and P. M. Rentzepis, *Science*, **194**, 276 (1976).
(26) M. A. El-Sayed, *Annu. Rev. Phys. Chem.*, **26**, 235 (1975).
(27) H. Levanon in "Multiple Electronic Resonance", M. Dorio and J. H. Freed, Ed., Plenum, New York, N.Y., 1978, Chapter 13, and references therein.
(28) S. G. Boxer and G. L. Closs, *J. Am. Chem. Soc.*, **97**, 3268 (1975).
(29) For a complete analysis of the triplet spin-Hamiltonian, see C. A. Hutchison, Jr., in "The Triplet State", A. B. Zahlan, Ed., Cambridge University Press, New York, N.Y., 1967, p 63.
(30) For a discussion on singlet–triplet mixing, see Chapter 5, in ref 17.
(31) K. H. Hausser and H. C. Wolf, *Adv. Magn. Reson.*, **8**, 85 (1976).
(32) W. G. Van Dorp, T. J. Schaafsma, M. Soma, and J. H. Van der Waals, *Chem. Phys. Lett.*, **21**, 47 (1973).
(33) A. L. Kwiram, *Chem. Phys. Lett.*, **1**, 272 (1967).
(34) J. Schmidt, I. A. M. Hasselmann, M. S. de Groot, and J. H. Van der Waals, *Chem. Phys. Lett.*, **1**, 434 (1967).
(35) M. Sharnoff, *J. Chem. Phys.*, **46**, 3263 (1967).
(36) R. H. Clarke and J. M. Hayes, *J. Chem. Phys.*, **59**, 3113 (1973).
(37) R. H. Clarke and R. H. Hofeldt, *J. Chem. Phys.*, **61**, 4582 (1974).
(38) W. G. Van Dorp, W. H. Schoemaker, M. Soma, and J. H. Van der Waals, *Mol. Phys.*, **30**, 1701 (1975). However, these authors show that a straight extrapolation may result in erroneous results because of the nonlinear dependence at low light intensities.
(39) Strictly speaking the total Hamiltonian should include the electron nuclear

interaction term and the nuclear Zeeman term. However, in this discussion of photoexcited triplets these terms are negligible.
(40) In fact, it is not a real $\Delta M_s = \pm 2$ transition because the spin wave functions at low fields differ from those at high fields. This transition will not be emphasized in this survey.
(41) For an exception see, A. M. P. Goncalves and R. P. Burgner, *J. Chem. Phys.*, **61,** 2975 (1974).
(42) For a discussion and references on EPR detection of randomly oriented triplets, see ref 17.
(43) The line shape represents the first derivative of the susceptibility χ'' with respect to the external magnetic field.
(44) M. A. El-Sayed and S. Siegel, *J. Chem. Phys.*, **44,** 1416 (1966).
(45) S. Siegel and H. S. Judeikis, *J. Phys. Chem.*, **70,** 2205 (1966). A different method for ZFS sign determination has been pointed out by El-Sayed.[26] This method utilizing the analysis of the ESP patterns combined with the determination of the sign of the *g* factor.
(46) Contrary to the OMR method where the measuring temperature is very critical (<4.2 K), ordinary triplet EPR spectra can be detected over a wide range of low temperature (for EPR detection at room temperature few examples have been also reported; see, for example, E. L. Frankevich et al., *Chem. Phys. Lett.*, **47,** 304 (1977); S. S. Kim and S. I. Weissman, *J. Mag. Res.*, **24,** 167(1976)).
(47) S. I. Weissman, *J. Chem. Phys.*, **29,** 1189 (1958).
(48) If this requirement is not satisfied, a first-order correction (in the zero-field Hamiltonian) should be added to the rate constants (see eq 5.39, p 158 in ref 49).
(49) N. M. Atherton in "Electron Spin Resonance, Theory and Applications", Wiley, New York, N.Y., 1973.
(50) H. Levanon and S. I. Weissman, *Isr. J. Chem.*, **10,** 1 (1972).
(51) H. Levanon and S. Vega, *J. Chem. Phys.*, **61,** 2265 (1974).
(52) M. Schwoerer and S. Sixl, *Z. Naturforsch.*, **249,** 952 (1969).
(53) J. F. Kleibeuker and T. J. Schaafsma, *Chem. Phys. Lett.*, **29,** 116 (1974).
(54) C. J. Winscom, *Z. Naturforsch.*, **309,** 571 (1975).
(55) S. J. Van der Bent, A. de Jager, and T. J. Schaafsmer, *Rev. Sci. Instrum.*, **47,** 117 (1976).
(56) C. C. Felix, S. S. Kim, and S. I. Weissman, *Chem. Phys. Lett.*, **48,** 29 (1977).
(57) R. A. Uphaus, J. R. Norris, and J. J. Katz, *Biochem. Biophys. Res. Commun.*, **61,** 1057 (1974).
(58) J. R. Norris, R. A. Uphaus, and J. J. Katz, *Chem. Phys. Lett.*, **31,** 157 (1975).
(59) M. C. Thurnauer, J. J. Katz, and J. R. Norris, *Proc. Natl. Acad. Sci. U.S.A.*, **72,** 3270 (1975).
(60) M. Cocivera, *Chem. Phys. Lett.*, **2,** 259 (1968).
(61) For a recent textbook on porphyrins see "Porphyrins and Metalloporphyrins", K. M. Smith, Ed., Elsevier, Amsterdam, 1975.
(62) I. Y. Chan, W. G. Van Dorp, T. J. Schaafsma, and J. H. Van der Waals, *Mol. Phys.*, **22,** 741, 753 (1971); also, the reader is referred to in W. G. Van Dorp, Thesis, Leiden, 1975.
(63) J. F. Kleibeuker, R. J. Platenkamp, and T. J. Schaafsma, *Chem. Phys. Lett.*, **41,** 557 (1976); also, the reader is referred to J. F. Kleibeuker, Thesis, Wageningen, 1977.
(64) R. H. Clarke, R. E. Connors, T. J. Schaafsma, J. F. Kleibeuker, and R. J. Platenkamp, *J. Am. Chem. Soc.*, **98,** 3674 (1976).
(65) R. H. Clarke, R. E. Connors, H. A. Frank, and J. C. Hoch, *Chem. Phys. Lett.*, **45,** 523 (1977).
(66) E. Nissani, A. Scherz, and H. Levanon, *Photochem. Photobiol.*, **25,** 93 (1977).
(67) M. C. Thurnauer and J. R. Norris, *Chem. Phys. Lett.*, **47,** 100 (1977).
(68) C. A. Hutchison and B. W. Mangum, *J. Chem. Phys.*, **29,** 952 (1958); **34,** 908 (1961).
(69) M. C. Thurnauer and J. R. Norris, *Biochem. Biophys. Res. Commun.*, **73,** 501 (1976).
(70) It is assumed that the molecular coordinate system coincides with the two $\pi\pi^*$ transitions Q_x and Q_y which are approximately perpendicular to each other in the molecular plane.[71]
(71) C. Weiss, Jr., *J. Mol. Spectrosc.*, **44,** 37 (1972).
(72) F. Metz, S. Friedrich, and G. Hohlneicher, *Chem. Phys. Lett.*, **56,** 4059 (1972).
(73) Notice, however, that the depopulation rates in zinc porphine are of the same order of magnitude (Table I). This difficulty has been noticed by Van Dorp et al.[38]
(74) M. K. Bowman, *Chem. Phys. Lett.*, **48,** 17 (1977).
(75) Y. Harel, J. Manassen, and H. Levanon, *Photochem. Photobiol.*, **23,** 337 (1976).
(76) D. Holten, M. Gouterman, W. W. Parson, M. W. Windsor, and M. G. Rockley, *Photochem. Photobiol.*, **23,** 415 (1976).
(77) M. Gouterman and D. Holten, *Photochem. Photobiol.*, **25,** 85 (1977).
(78) J. Franck and J. L. Rosenberg, *J. Theor. Biol.*, **7,** 276 (1964).
(79) D. L. Dutton, J. S. Leigh, and M. Seibert, *Biochem. Biophys. Res. Commun.*, **46,** 406 (1972).
(80) J. S. Leigh and D. L. Dutton, *Biochem. Biophys. Res. Commun.*, **46,** 414 (1972).
(81) J. S. Leigh and D. L. Dutton, *Biochim. Biophys. Acta*, **357,** 67 (1974).
(82) D. L. Dutton, J. S. Leigh, and D. W. Reed, *Biochim. Biophys. Acta*, **292,** 654 (1973).
(83) Optical evidence for triplet states in bacteria was also provided by M. Seibert and D. Devault, *Biochim. Biophys. Acta*, **253,** 396 (1971).
(84) M. Y. Okamura, R. A. Isaacson, and G. Feher, *Proc. Natl. Acad. Sci. U.S.A.*, **72,** 3491 (1975).
(85) A. A. Krasnovskii, Jr., N. N. Lebedev, and F. F. Litvin, *Dokl. Akad. Nauk SSSR*, **216,** 1406 (1974).
(86) A. W. H. Mau and M. Puza, *Photochem. Photobiol.*, **25,** 601 (1977).
(87) S. Boxer and G. Closs, private communication.
(88) W. W. Parson, R. K. Clayton, and R. J. Cogdell, *Biochim. Biophys. Acta*, **387,** 265 (1975).
(89) R. C. Prince, J. S. Leigh, and P. L. Dutton, *Biochim. Biophys. Acta*, **440,** 622 (1976).
(90) A. J. Hoff, *Biochim. Biophys. Acta*, **440,** 765 (1976).
(91) R. H. Clarke, R. E. Connors, J. R. Norris, and M. C. Thurnauer, *J. Am. Chem. Soc.*, **97,** 7178 (1975).
(92) R. H. Clarke and R. E. Connors, *Chem. Phys. Lett.*, **42,** 69 (1976).
(93) S. J. Van der Bent, T. J. Schaafsma, and J. C. Goedheer, *Biophys. Biochem. Res. Commun.*, **71,** 1147 (1976).
(94) J. R. Norris and M. C. Thurnauer, *Biophys. J.*, **16,** 224a (1976), Abstract F-PM-D11.
(95) J. R. Norris and M. C. Thurnauer in International Seminar on Excitation Transfer in Condensed Matter, Prague, Czechoslovakia, 1976.
(96) At a constant separation because of the $1 - 3\cos^2\theta$ factor, the end-to-end interaction is twice as strong and opposite in sign to the side-by-side interaction.
(97) For general reviews see "Chemically Induced Magnetic Polarization", A. R. Leplay and G. L. Closs, Ed., Wiley, New York, N.Y., 1973.
(98) For a recent review on CIDEP see P. W. Atkins and G. T. Evans, *Adv. Chem. Phys.*, **35,** 1 (1976).
(99) We use the notation of $(Bchl)_2^{\cdot+}Bph^{\cdot-}$ pair for generalization. The reader should be aware of the fact that the identity of the anion half is not completely settled.
(100) R. K. Clayton and T. Yamamoto, *Photochem. Photobiol.*, **24,** 67 (1976).
(101) F. K. Fong, *J. Am. Chem. Soc.*, **98,** 7840 (1976).
(102) Fong interprets the observed triplet as significantly involved with P_{800} on grounds of optical changes of P_{800} during the lifetime of P^R.
(103) J. J. Katz and J. R. Norris in "Current Topics in Bioenergetics", Vol. 5, Academic Press, New York, N.Y., 1973, p 41.
(104) F. K. Fong, *Appl. Phys.*, **6,** 151 (1975).
(105) L. L. Shipman, T. M. Cotton, J. R. Norris, and J. J. Katz, *Proc. Natl. Acad. Sci. U.S.A.*, **73,** 1791 (1976).
(106) R. M. Hochstrasser and T. S. Lin, *J. Chem. Phys.*, **49,** 4929 (1968).
(107) The interlink between the functional groups in the dimer depends on the water content in the solution: F. K. Fong, V. J. Koester, and L. Galloway, *J. Am. Chem. Soc.*, **99,** 2372 (1977).
(108) A. J. Hoff and J. H. Van der Waals, *Biochim. Biophys. Acta*, **423,** 615 (1976).
(109) A. J. Hoff, Govindjee, and J. C. Romijn, *FEBS Lett.*, **73,** 191 (1977).
(110) R. Blankenship, A. McGuire, and K. Sauer, *Proc. Natl. Acad. Sci. U.S.A.*, **72,** 4943 (1975).
(111) K. H. Sauer, R. H. Blankenship, G. C. Dismukes, and A. McGuire, *Biophys. J.*, **17,** Abstract F-AM-F2 (1977).
(112) C. Dismukes, R. Friesner, and K. Sauer, *Biophys. J.*, Abstract F-AM-F3 (1977).
(113) A. R. McIntosh and J. R. Bolton, *Nature (London)*, **263,** 443 (1976).
(114) A net emission effect is possible (up to 5%) by RP mechanism via $|S\rangle \leftrightarrow |T_{-1}\rangle$ mixing.[98] Thus, it is unlikely that this type of mechanism will account for this observation.
(115) R. E. Blankenship, T. J. Schaafsma, and W. W. Parson, *Biochim. Biophys. Acta*, **461,** 297 (1977).
(116) A. J. Hoff, H. Rademaker, R. Van Grondelle, and L. N. M. Duysens, *Biochim. Biophys. Acta*, **460,** 547 (1977).
(117) R. H. Clarke, R. E. Connors, and J. Keegan, *J. Chem. Phys.*, **66,** 358 (1977).
(118) T. L. Netzel, P. M. Rentzepis, D. M. Tiede, R. C. Prince, and P. L. Dutton, *Biochim. Biophys. Acta*, **460,** 467 (1977).
(119) J. S. Connolly, D. S. Gorman, and G. R. Seely, *Ann. N.Y. Acad. Sci.*, **206,** 649 (1973).
(120) T. Mar and G. Gringas, *Biochim. Biophys. Acta*, **440,** 609 (1976).
(121) V. A. Shuvalov, A. A. Asadov, and J. N. Krakhmaleva, *FEBS Lett.*, **76,** 240 (1977).
(122) A. J. Anton, J. Kwong, and P. A. Loach, *J. Heterocycl. Chem.*, **13,** 717 (1976).
(123) S. G. Boxer and G. L. Closs, *J. Am. Chem. Soc.*, **98,** 5406 (1976).
(124) M. R. Wasielewski, M. H. Studier, and J. J. Katz, *Proc. Natl. Acad. Sci., U.S.*, **73,** 4282 (1976).